

Scanning probe microscopy at video-rate

Recent results have demonstrated the feasibility of video-rate scanning tunneling microscopy and video-rate atomic force microscopy. The further development of this technology will enable the direct observation of many dynamic processes that are impossible to observe today with conventional Scanning Probe Microscopes (SPMs). Examples are atom and molecule diffusion processes, the motion of molecular motors, real-time film growth, and chemical or catalytic reactions. Video-rate scanning probe technology might also lead to the extended application of SPMs in industry, e.g. for process control. In this paper we discuss the critical aspects that have to be taken into account for improving the imaging speed of SPMs. We point out the required instrumentation efforts, give an overview of the state of the art in high-speed scanning technology and discuss the required future developments for imaging at video-rates.

Georg Schitter

*Delft Center for Systems and Control, Delft University of Technology, Mekelweg 2, 8c-3-22, 2628 CD Delft, The Netherlands,
E-mail: g.schitter@tudelft.nl*

Marcel J. Rost

*Leiden University, Leiden Institute of Physics, P.O. Box 9504,
2300 RA Leiden, The Netherlands
E-mail: rost@physics.leidenuniv.nl*

In 1981 Binnig *et al.* invented the scanning tunneling microscope (STM)¹, which enables a (semi)conducting surface to be imaged with atomic resolution. Based on this first scanning probe microscope (SPM) and driven by the wish to also image non-conductive surfaces, Binnig *et al.* went on to invent the Atomic

Force Microscope (AFM) in 1986². A variety of other SPMs have since been developed, such as the Electrochemical STM (EC-STM)³, the scanning near-field optical microscope (SNOM)⁴, the scanning ion-conductance microscope⁵, the scanning capacitance microscope⁶ and the magnetic force microscope⁷.

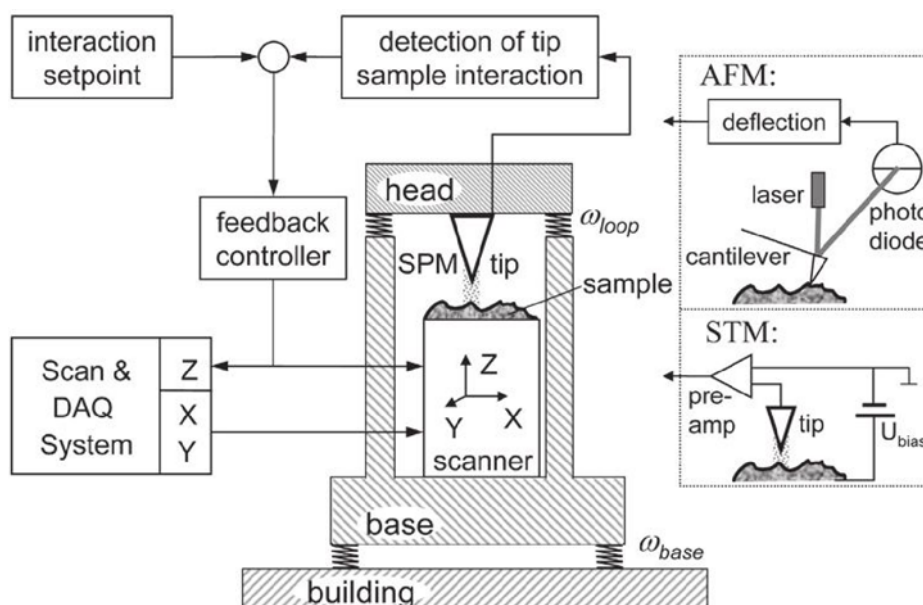


Fig. 1 Scheme of a standard SPM system, showing the scanner (X- and Y-directions) and the feedback loop that keeps the tip–sample interaction constant (Z-direction). The detection of the signals for feedback operation is shown in the inserts to the right for AFM and STM, respectively.

The principle of all SPMs is probing the interaction between the sample surface and a sharp tip (see Fig. 1), while either of them is scanned laterally in the area of interest. In the STM this tip–sample interaction is the tunneling current¹, whereas in the AFM it is the forces acting between the tip and the sample surface^{2,8}. For most SPM modes this tip–sample interaction is held constant by a feedback loop that varies the vertical (Z) position between the sample and the tip in order to compensate for variations in the tip–sample interaction, such as those induced by the sample topography during the scanning process.

This task requires a positioning unit (the so-called SPM scanner) that allows movement in all three spatial directions with (sub-) nanometer resolution. By simultaneously recording both the relative lateral position of the tip with respect to the sample and the feedback action that maintains a constant tip–sample interaction, a three-dimensional surface map of the measured sample property is drawn. This corresponds to the most common imaging modes in both the STM and the AFM, measuring the density of electronic states and the surface topography, respectively.

As well as imaging the surface topography with molecular and even (sub-)atomic resolution^{1,9–11}, modern SPMs also allow direct measurements of local sample properties with high spatial resolution, such as Young's modulus and surface adhesion¹², friction^{13–16}, charge distribution¹⁷, electronic local density of states^{18,19} and magnetic states^{20,21}. In addition, SPMs are also used, for example, for single molecule spectroscopy²², data storage^{23,24} and nanolithography^{25,26}, and as a nanorobot to manipulate single nanoparticles, molecules and even individual atoms^{27–29}. The continued development of SPM technology by various research groups both in academia and industry constantly enables new measurement methods and greater precision.

Although SPM technology is very versatile, the main advantage of its high resolution is diminished by the inherently limited temporal resolution. In this paper we highlight those technological developments that we believe are feasible in the near future, and that will enable the same accurate control of the tip–sample interaction at high imaging speeds as is currently achievable with SPMs only when measuring in standard (slow) imaging mode. In view of this, we discuss the latest developments in high-speed SPM imaging that, in combination, may introduce the next generation of video-rate SPMs.

Video-rate scanning probe microscopy will have a major impact on the understanding of numerous open questions in the fields of materials science^{30,31}, chemistry and biology^{32,33}. As examples, one might think of surface diffusion, phase transition, self-assembly phenomena, film growth and etching, chemical processes and catalytic reactions, biomineralization, and biomolecular motors and processes. Video-rate SPM technology will also make the use of SPMs more accessible for industrial applications, e.g. in serial production and process control.

High-speed scanning probe microscopy

The most probably explanation for the slow-down in development of SPM systems in the mid-1990s is that almost all the components of an SPM were well matched with regard to performance and pushed close to their limits. There was not a single bottleneck in terms of speed, implying that any improvement would entail the replacement of almost every component of the SPM. Such improvement would require detailed knowledge of all the involved disciplines, such as physics, mechanics and electronics, to overcome the limitations and to develop an integrated new SPM system.

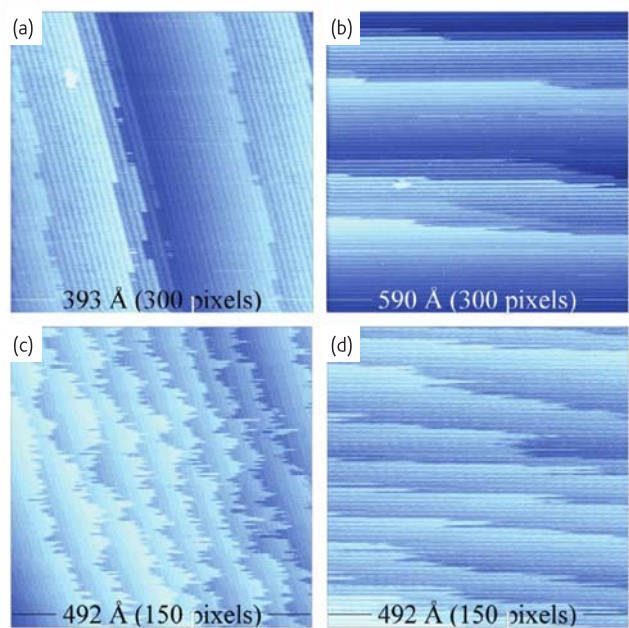


Fig. 2 STM images (tunneling parameters: $V = -0.7\text{ V}$, $I < 0.1\text{ nA}$) of step structures on Au(110). The steps appear totally different when imaged with different time resolutions. The upper panels were taken at a temperature of 384 K and the lower panels at 479 K. The two left panels were measured in 31 s (a) and 21 s (c) in a scan orientation nearly perpendicular to the step direction. In the two right panels, 31 s (b) and 5 s (d), the scans were repeated at the same location, with an orientation roughly parallel to the steps, in order to optimize the time resolution. The fuzzy-looking step structures in the two left panels are not real, but merely result from rapid kink motion along the steps⁶².

Pioneering work demonstrated significant improvements in SPM technology, and the possibility for higher imaging rates in particular. By 1986 Bryant *et al.* were already reporting on real-time STM imaging in constant-height mode with line frequencies beyond 1 kHz³⁴. Since then, several groups had pushed the STM technology forward in order to generally increase the imaging rate^{35–52}. The diffusion study of individual atoms on a surface, however, required an even higher

temporal resolution than 20 images per second, which was achieved in 1992 by Ludwig *et al.*³⁶. Therefore, Swartzentruber realized the first atom-tracking STM⁵³ in 1996, inspired by the surface tracking method proposed in 1988⁵⁴. Since Swartzentruber, several groups have applied this technique in order to reach the necessarily higher temporal resolution for diffusion studies of individual atoms, atom clusters and molecules^{55–60}. However, this technique involves following only the feature of interest, so one is blind not only to the tracking feature but also to any surface changes that might influence the diffusion. In order to ensure that the diffusion process is interpreted correctly, it is important to measure complete images at high frame rates, thereby also capturing any changes in the surrounding surface area. Such studies might become possible in the future: constructing a rigid scanner and realizing the so-called hybrid mode enabled images to be obtained at 10,000 lines per second⁶¹ while still keeping atomic resolution. Fig. 2 demonstrates the potential for misinterpretation when imaging with a limited time resolution. The fuzzy-looking step structures are not real but merely result from the mobility of atoms along the steps⁶².

Concerning AFMs, one major improvement for imaging speed was the development of small cantilevers by the Hansma laboratory^{63,64}. AFM cantilevers with smaller dimensions enable higher imaging speeds^{32,65,66}, as they have higher resonance frequencies in combination with a sufficiently low cantilever stiffness.

The introduction of small, and therefore fast, actuators for the vertical displacement^{67–69} significantly improved the feedback bandwidth for tracking the tip-sample interaction using piezoelectric actuation⁷⁰ or thermal actuation of an AFM cantilever⁷¹. Another approach is the construction of more rigid scanners^{32,61,72,73}, as they enable the scanning unit to respond more quickly. Further considerable speed improvements have been achieved by applying modern control methods to the SPM scanner for lateral scan displacements^{74–76}, as well as for the Z-displacement that is controlled by the feedback system^{77–80}.

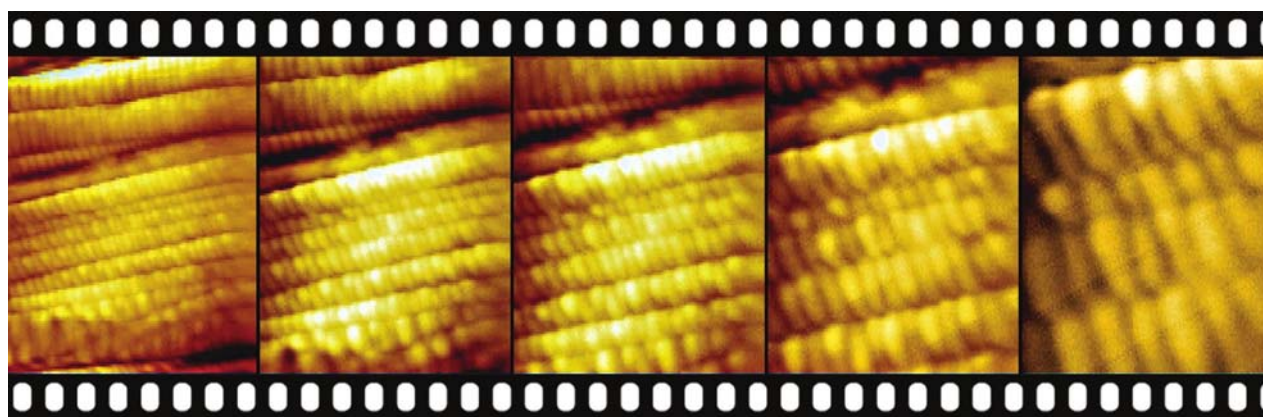


Fig. 3 This series of images of rat tail collagen illustrates how video-rate AFM allows rapid zooming in on areas of interest. The entire zoom series from an image width of 2 μm to a width of 470 nm was taken in 0.56 s and shows every fourth image in the series. The collagen's characteristic 67 nm banding pattern is clearly resolved in the raw data and enhanced with image processing for easy visibility. A conventional AFM would need about 15 min of imaging to obtain a comparable series of images. Reprinted from⁶⁶ with permission from AAAS.

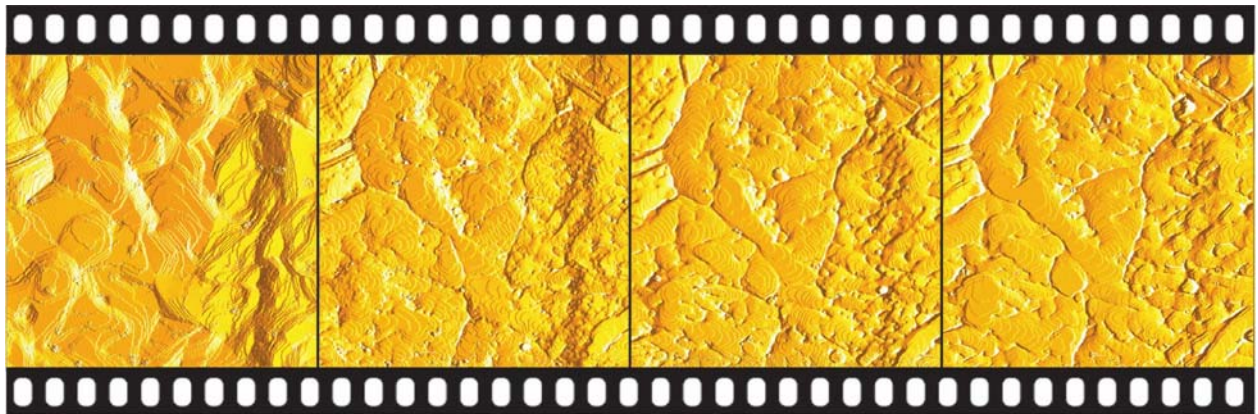


Fig. 4 An example of an *in situ* real-time observation of the deposition of a thin polycrystalline gold film. The four STM images ($495 \times 495 \text{ nm}^2$) were taken from a movie that was recorded during the deposition while continuously scanning with the microscope³¹, with permission from AAAS

Integrating some of the above improvements, Ando *et al.*³² reported the first AFM system that could image at more than 1000 lines per second³², enabling the direct observation of biomolecular processes³³. Other than the bandwidth for detection of the tip-sample interaction, the key issue for video-rate SPM is the mechanical design and control of the SPM scanner. Hansma *et al.*^{66,73} recently reported an AFM system with video-rate imaging capabilities (cf. Fig. 3) at a scan range of more than $10 \mu\text{m}$ and a Z-feedback bandwidth on the order of 100 kHz. Instead of building rigid scanners, Miles's group used the scanner resonance for performing the scanning motion⁸¹. With this method, imaging rates of 30,000 lines per second have been reported for SNOM⁸² and 100,000 lines per second for a recent AFM system⁸³. Although this solution enables very fast scanning, the tip-speed and thus the pixel resolution varies over the image, with the lowest resolution and highest speed in the image center. It is important to note that the height data may be influenced by the varying feedback response due to the varying speed. If one records deflection data only, larger and perhaps harmful variations of the tip-sample forces may occur. In view of this, it is interesting to note that at extremely high line-rates it is possible to observe a relatively soft biological specimen in contact mode AFM without causing any discernible damage⁸³. Figs. 3 and 4 demonstrate the power of video-rate imaging with two recent SPM prototypes, demonstrating AFM imaging of a biological

sample⁶⁶ and direct observation of a film growth process with an STM³¹, respectively.

Requirements for Video-Rate SPM

The bandwidth requirements for the individual SPM positioning axis for video-rate imaging are listed in Table 1 (cf. Fantner *et al.*⁸⁴). It is hard to directly compare the recently reported video-rate SPM systems^{32,61,66,81}, as they are often designed for a particular application, implying specific advantages and disadvantages in terms of scan range, resolution and imaging speed. For example, a scan range of typically a few hundreds of nanometers and a Z-range of a few tens of nanometers is sufficient for high-speed imaging of individual biomolecular processes at high spatial and temporal resolutions (see Ando *et al.*³³). A similar positioning range with an even higher spatial resolution is required for video-rate STM when intended for imaging atomic processes^{30,31} (cf. Figs. 4 and 7). The set of specifications may be completely different when aiming to image larger systems, such as cells^{85,86}. On the one hand, this requires a larger scan size ($>10 \mu\text{m}$) and Z-range; on the other hand, the demand on the temporal resolution may be less compared to, say, the imaging of molecular motors.

It is a challenge to develop instrumentation that could increase the imaging speed of conventional SPMs by more than two orders of magnitudes, as this implies an increase in the bandwidth of several

Table 1 Bandwidth requirements for the individual positioning axis for video-rate SPM⁸⁴

	Video-rate SPM	High-speed SPM	Intermediate speed
Pixel resolution	256 x 256 pixel	256 x 256 pixel	100 x 100 pixel
Frame rate	25 frames/s	10 frames/s	10 frames/s
Scan requirements			
Z-direction	3.3 MHz	1.3 MHz	200 kHz
X-direction	6.4 kHz	2.6 kHz	1 kHz
Y-direction	12.5 Hz	5 Hz	5 Hz

If the scanning motion is performed in the predominant triangular scan pattern, the requirements for the X- and Y-directions increase by about one order of magnitude. If image rotation is desired for the scan, the requirement for the Y-direction has to be the same as defined for the X-direction.

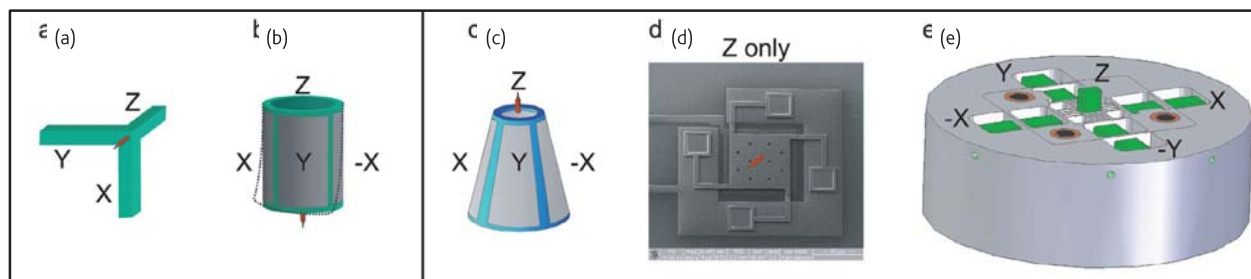


Fig. 5. Different scanner geometries: (a) the early tripod; (b) the tube that is still used in most SPM instruments. Recently developed improved scanners: (c) the cone⁹⁰; (d) a MEMS Z-stage⁹⁰; and (e) a flexure-based scanner⁷³.

key components without compromising on the resolution of the microscope. The mechanical components have to meet demanding specifications to achieve the required bandwidth, which eventually might imply the use of Microelectromechanical systems (MEMS; see Fig. 5). Furthermore, the significantly increased noise accumulated in the imaging system at a thousandfold bandwidth puts stringent demands on the electronics involved in the imaging process.

The main speed-limiting factors in today's SPM systems are:

1. the dynamic behavior of the scanner;
2. the bandwidth of the power amplifiers that drive the piezoelectric actuators;
3. the bandwidth for detection of the tip-sample interaction at a sufficient signal-to-noise ratio;
4. the dynamic behavior of the SPM probe: AFM cantilever and special tips, such as carbon nanotubes or insulated STM tips for EC-STM;
5. the bandwidth of the feedback control system; and
6. the speed of the data acquisition system.

The main resolution limiting factors are:

1. the noise floor of the power amplifiers;
2. the detection noise of the tip-sample interaction (cantilever deflection in AFM and tunneling current in STM);
3. the nonlinearity and dynamic coupling between the positioning axis of the SPM scanner; and
4. disturbances, such as mechanical and acoustical vibrations that cause image distortions.

Mechanical design

Video-rate SPM requires a fast response of the scanner, which calls for a high first resonance frequency of the mechanical components. Here, we have to distinguish between the system components that are part of the active control loop, such as the scanner and the power amplifiers, and the components that form the passive mechanical loop between the tip and the sample (see Fig. 1). While the dynamics of the components in the control loop determine the maximum bandwidth for active positioning, and thus imaging, the achievable imaging bandwidth is not directly

limited by the resonance frequencies of the passive mechanical loop (see ω_{loop} in Fig. 1). However, as excitation of the latter may significantly distort the SPM images, these resonances should also be considered in the SPM design. In addition, the SPM must be effectively decoupled from external vibrations⁸⁷ by a suspension system with a low resonance frequency ω_{base} (see Fig. 1) and low damping. For all frequencies $\omega > \omega_{base}$, the amplitude of the external vibrations coupling into the base decay with $(\omega/\omega_{base})^{-2,88}$. Therefore one desires an anti-vibration stage with a resonance frequency as low as possible. In contrast to the suspension system, the mechanical loop between the tip and the sample (see ω_{loop} in Fig. 1) should be as stiff as possible. In the optimal case, ω_{loop} is even higher than the imaging bandwidth. In this case ($\omega_{base} \ll \omega \ll \omega_{loop}$), mechanical vibrations within the SPM that are induced by the displacement of the scanner (any displacement of a piezo causes reaction forces) will not excite the structural dynamics between the tip and the sample. Although desirable, the nature of the SPM makes it impossible to construct an infinitely rigid mechanical loop, as its operation requires an approach mechanism between the tip and the sample, i.e. moving parts within the mechanical loop. Unfortunately, this resonance frequency is rather low for piezo motors, as well as for micrometer screws (typically on the order of single kHz), when compared with the imaging bandwidth of recent SPM prototypes that have reached displacements on the order of 100 kHz and beyond⁸⁰. As video-rate imaging implies even higher frequencies, future improvement in the stiffness of the approach mechanism is needed.

When the induced vibrations due to scanning signals and Z-motion approach ω_{loop} , one has to ensure that the amplitudes stay within the noise floor of the SPM. This is possible by increasing the mass ratio between stationary parts (the base) and the moved parts, e.g. by using MEMS-based devices, or by generating a corresponding counterforce, e.g. with a balanced actuator that avoids coupling of any vibrations into the base-head structure.

Another important design consideration is the dynamic coupling between the individual positioning axes of the scanner itself, as the scanning in the X- and Y-directions can cause severe image distortion due to the coupling in the Z-direction^{61,75}. However, it is possible to compensate for this effect by utilizing modern control methods (discussed later), as this is part of the active components.

Another aspect that has to be considered in the design of the video-rate SPM is the initiation of processes to be imaged at video-rate. This not only depends on the SPM mode and imaging application, but also requires the capability, for example, of liquid exchange to trigger biological processes, or temperature and environmental control in case of crystal growth processes.

Tube scanner/cone scanner

After using tripod scanners¹ in the first SPMs, Binnig and Smith invented a four-segmented, single piezo-tube scanner in 1986⁸⁹ in order to image faster with less image distortion (see Fig. 5a and b). The benefits are obvious: tube scanners provide a very good ratio between accessible scan range and resonance frequency. This concept is still widely used today in conventional SPMs, enabling scan ranges of more than 100 μm with the first resonance frequency on the order of 1 kHz, or a scan range of a few microns with the first resonance on the order of 10 kHz. The capability for video-rate scanning largely depends, therefore, on the desired scan range and the application.

Based on the tube scanner, a conical piezo geometry (see Fig. 5c) has been developed recently⁹¹ that has two main advantages over the tube piezo. First, the triangular aspect of this shape makes the structure stiffer, since the triangular cross-sections are hard to bend or shear. Secondly, the mass of the moving parts is reduced, taking into account a larger reduction for parts that move with a larger amplitude. This results in a scanner with even higher resonance frequencies (47 kHz in the X- and Y-directions, and 70 kHz in the Z-direction), while simultaneously keeping a sufficiently large scan range (800 × 800 × 400 nm³).

An even greater increase in the resonance frequency can be achieved by the application of MEMS scanners. Recently a MEMS Z-stage (see Fig. 5d) has been realized, with a positioning range of about 300 nm and a first resonance frequency of 170 kHz⁹².

Flexure scanners

In the case where a relative large mass has to be moved, e.g. when the sample is scanned, one requires a scanner structure with a high stiffness⁷² in order to maintain a high resonance frequency. In addition, the rapid acceleration of the larger mass requires an actuator that provides a high force. This can be realized by using piezoelectric stack actuators. Different mechanical designs have been reported in the literature that combine individual piezo-stacks to a three-dimensional SPM scanner (see Fig. 5e), where the actuation can be realized in either a serial³² or parallel manner^{72,93}. Flexure-based scanners with first resonances beyond 20 kHz enable video-rate imaging (cf. Fig. 3) at a scan range of more than 10 μm ⁷³.

Scanning motion

The operation of an SPM system can be split into two main parts: (i) performing the scanning motion; and (ii) controlling the tip-sample interaction during the imaging process. Although these two positioning

problems are not fully decoupled, we will treat them separately in the following.

Power amplifiers

As mentioned in the last section, SPM imaging at video-rate requires a high first mechanical resonance frequency of the scanner (including the piezo actuators). This also implies that one needs to drive the scanning piezos at a high bandwidth without sacrificing the resolution, i.e. the positioning noise. While tube and cone scanners have moderate capacitances (on the order of a few nanofarads), piezo-stacks put a high demand on the power amplifiers, as their capacitance is typically about two to three orders of magnitudes larger. The application of piezo-stacks for video-rate imaging necessarily calls for custom-made amplifiers that are optimized for the specific capacitive load of the corresponding piezo^{32,93}.

Control of the scanning motion

The scanning motion is typically performed following a triangular signal, in order to achieve a constant tip-sample velocity during the imaging process and a constant pixel distance when recording the data^{61,84}. However, hysteresis and creep of the scanning piezos as well as the resonances of the SPM may distort the scanning motion, causing imaging artifacts, particularly at high speed⁹⁴. Modern control technology has demonstrated a significant reduction in several imaging artifacts introduced by the scanner nonlinearity and dynamics, where one has to distinguish between open-loop and closed-loop control. If the scanner is equipped with X- and Y-position sensors, feedback control can be used to eliminate both hysteresis and creep⁷⁶, as well as to dampen the scanner resonances⁹⁵. However, feedback control for closed-loop scanning also has disadvantages. First, the closed-loop bandwidth is limited by the system dynamics^{76,77}; and, secondly, the positioning resolution may deteriorate due to feeding back of the sensor noise.

Hysteresis effects can be reduced in open-loop scanning⁷⁴ by pre-shaping the scanning signals or by driving the piezos with charge-controlled amplifiers⁹⁵. Creep can be diminished by implementing an inverse creep model⁷⁴ or, more effectively, an image-tracking algorithm⁹⁶ to control the offset on the scanning piezos. Resonances of the X- and Y-scanners can be suppressed by model-based filtering^{74,75} or via input-shaping techniques⁹⁷. A recently reported method based on iterative learning control^{98–100} combines the advantages of both open- and closed-loop control by optimizing the scanning signals using the position sensor information obtained during previous scanning cycles. As the optimized scanning signal is applied in an open-loop manner, it overcomes the above-mentioned drawbacks of closed-loop control.

SPM feedback of the tip-sample interaction

High-speed scanning necessarily requires a high bandwidth of the feedback loop to track the tip-sample interaction (see Fig. 6).

When operating the SPM with a slow feedback (low closed-loop bandwidth), more information is visible in the error image instead of the height image (cf. Hansma *et al.*⁶⁶). This may result in crashing or damaging the tip and deforming or destroying the (delicate) specimen.

The achievable bandwidth of the feedback loop depends on the dynamics of all the components within the loop¹⁰¹, i.e. the detection of the tip-sample interaction, the feedback system, the bandwidth of the power amplifier and the dynamics of the scanner in Z-direction^{32,77}. All the components must be carefully designed in order to push this bandwidth as high as possible. Considering video-rate imaging with all information in the height signal, one would need a bandwidth beyond 1 MHz (see Table 1). This bandwidth is still significantly higher than those reported in the literature to date^{61,71,79,80}, implying that for current video-rate SPMs both height and error images are required to provide full surface information.

Probing the tip-sample interaction

Tracking the tip-sample interaction at high bandwidth naturally requires its detection at a corresponding high bandwidth.

For video-rate STM one has to measure a signal that corresponds to the tunneling current with a sufficiently high bandwidth in combination with low noise. In the sensing circuit of the feedback we can identify two critical components that are currently limiting the maximum possible bandwidth: the preamplifier and the logarithmic converter. As the noise of electronic amplifiers increases at least with the square root of the bandwidth, the major problem is measuring the tunneling current at high frequencies while simultaneously keeping the noise in the picoampere regime⁹⁰. For example, the atomic frequency of

the image shown in Fig. 7 is approximately 350 kHz, obtained with a sufficiently low-noise preamplifier that operates up to 600 kHz⁶¹.

When applying STM-MEMS scanners^{90,92}, another challenge arises: in order to avoid coupling of the actuation signals into the tunneling current, care has to be taken to design proper shielding.

Video-rate AFM requires the detection of the cantilever deflection at a high bandwidth^{33,73} and with a sufficiently large signal-to-noise ratio. The signal for feedback operation depends on the imaging mode, i.e. the deflection signal for contact mode and the amplitude of the oscillating cantilever for tapping mode. In both cases the response time of the AFM cantilever scales with the cantilever resonance, which may limit the imaging speed. For contact mode, one requires cantilevers with a resonance frequency beyond the feedback bandwidth. For tapping mode, one needs cantilevers with exceptionally high resonance frequencies (on the order of 1 MHz and beyond)⁷¹, as the response time of the tapping cantilever depends not only on the resonance frequency but also on the quality factor. As mentioned above, small cantilevers have proven to be very useful for tapping mode at high speeds, as they enable high resonance frequencies at relative low stiffness for gentle imaging. However, further improvement in cantilever technology, as well as fast demodulation of the tapping signal, is required to push the limits of the current force probes even further, thus enabling even higher imaging rates.

Feedback system

Conventional SPM systems typically use a Proportional-Integral (PI) element as feedback to control the tip-sample interaction. Significant improvements in imaging bandwidth have been demonstrated by replacing the standard PI feedback controller by a model-based

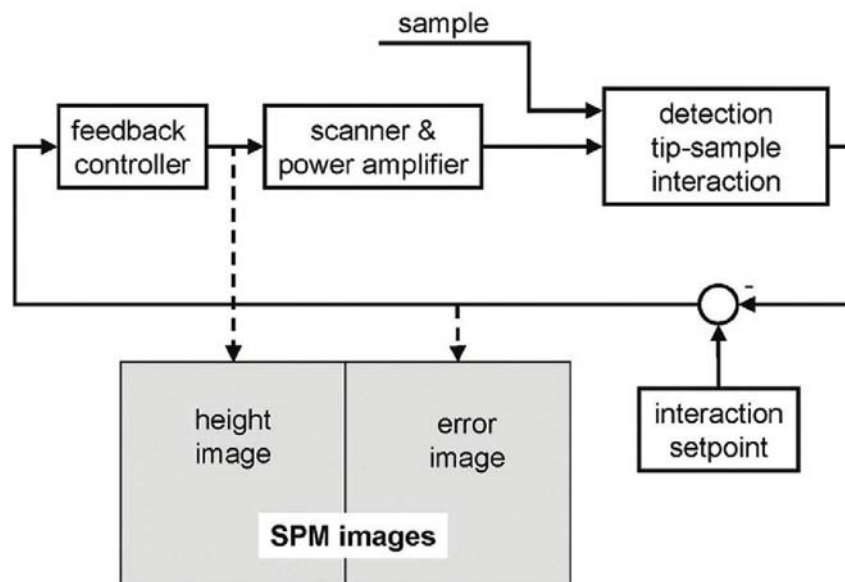


Fig. 6 SPM feedback loop to track the tip-sample interaction in the Z-direction (height). Proper feedback control implies as much information as possible in the height image with as little as possible in the error image.

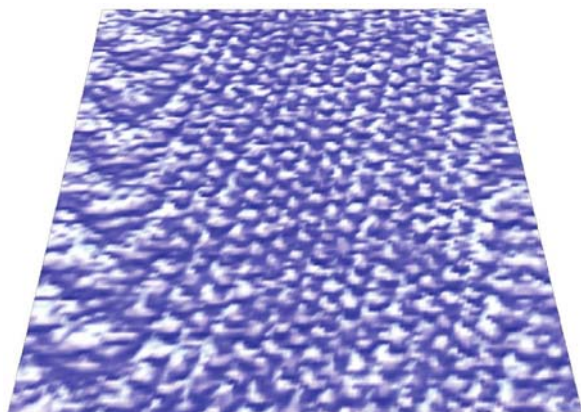


Fig. 7 STM image of an HOPG surface showing atomic resolution. The image (128×128 pixels) is obtained with a line rate of ~ 10 kHz and a frame rate of 80 images per second at a tunneling current of $I = 1$ nA and a sample voltage of $U_s = -0.1$ V⁶¹. The distortion at the edges is due to rounding of the scan signals and hysteresis of the piezo element.

controller^{77,80}, by applying active damping to the piezo element⁷⁸ in addition to the PI feedback, by adapting the PI feedback as a function of the actual operation point⁷⁹, which corresponds to a gain scheduling approach, and by feeding forward¹⁰² the topographic information obtained from previous scan lines. Furthermore, a model-based approach^{77,103} also allows a more accurate estimate of the sample profile as compared to recording just the feedback signal as height information, which is standard in conventional SPM controllers.

Coupling

As mentioned above, dynamic cross-coupling between the individual positioning axes of the SPM scanner as well as mechanical vibrations of the SPM structure due to the scanner displacement can cause several image distortions during video-rate imaging. The multiple frequency components of the scanning signals may, in combination with the actuator nonlinearities, excite the dynamic cross-coupling of the SPM, as recently proven experimentally⁹⁰. Reduction and compensation⁹⁹ of these coupling-induced vibrations is one focus of future instrumentation efforts, as this may be required to achieve distortion-free video-rate SPM imaging.

Challenges


In our opinion, the most demanding and open questions for instrumentation of video-rate SPMs are achieving a higher feedback bandwidth combined with large displacement in the Z-direction (cf. Hansma *et al.*⁶⁶) and reducing the coupling between the individual positioning axes and the SPM structure, as these still cause significant image distortions.

First, one needs to improve the information content in the height signal as compared to the error signal (cf. Fig. 6). This step is necessary to allow gentle imaging at minimal tip-sample interaction forces and will result in more reliable (quantitative) measurement data. This challenge inherently requires both the development of faster actuators, potentially MEMS-based scanners⁹⁰ or directly actuated probes^{70,71}, and a higher detection bandwidth of the tip-sample interaction. For tapping mode AFM, faster cantilevers as well as fast demodulation of the cantilever oscillation at a sufficient signal-to-noise ratio is still a challenge that needs to be overcome. In STM, the challenge is to produce a large bandwidth preamplifier with sufficiently low noise.

Secondly, as the imaging spectrum may contain all frequencies up to the feedback bandwidth plus additional components generated by the (nonlinear) actuation, future developments also have to focus on improving the mechanical and control design. The aim is to minimize the nonlinearities and coupling-induced oscillations of the scanner as well as of the SPM structure, as an accurate as possible control of the scanning motion is a key factor for distortion-free SPM imaging at video-rate.

Conclusion

Recent laboratory prototypes have proven the feasibility of SPM imaging at video-rate. Several important improvements have been demonstrated, but an integrated SPM system that combines all aspects in one set-up still has to be developed. Moreover, in order to make video-rate SPMs more reliable, easier to use and even suited for commercialization, the technique still needs a significant amount of development and engineering. Here, the key challenges are to develop faster sensing of the tip-sample interaction and improve the imaging bandwidth (feedback) in the vertical direction, which is necessary to achieve a better control over the tip-sample interaction; and to improve the control of the (nonlinear) coupling between the individual positioning axis and the structural dynamics of the SPM. The development of even faster scanning units will allow further improvements in the temporal resolution of SPMs, even beyond video-rate. We hope to stimulate researchers from a range of disciplines, as the problems present interesting research challenges for the next few years in mechanical, electronics and control design.

Eventually, we expect that video-rate SPM will have a significant impact in the life- and materials sciences, since it will enable the investigation of dynamic processes on the molecular and atomic levels as they occur in nature. One can also foresee the increased application of video-rate SPM technology in industry, e.g. in process technology, quality control or even data storage. 

REFERENCES

1. Binnig, G., *et al.*, *Phys. Rev. Lett.* (1982) 49, 57.
2. Binnig, G., *et al.*, *Phys. Rev. Lett.* (1986) 56, 930.
3. Sonnenfeld, R. and Hansma, P. K., *Science* (1986) 232, 211.

4. Pohl, D. W., *et al.*, *Proc. SPIE* (1988) 897, 84.
5. Hansma, P. K., *et al.*, *Science* (1989) 243, 641.
6. Zavyalov, V. V., *et al.*, *Rev. Sci. Instrum.* (1999) 70, 158.
7. Hug, H. J., *et al.*, *Rev. Sci. Instrum.* (1993) 64, 2920.
8. Sarid, D., *Scanning Force Microscopy: With Applications to Electric, Magnetic, and Atomic Forces*, Oxford University Press, Oxford, (1994).
9. Binnig, G., *et al.*, *Phys. Rev. Lett.* (1983) 50, 120.
10. Drake, B., *et al.*, *Science* (1989) 243, 1586.
11. Giessibl, F. J., *Rev. Mod. Phys.* (2003) 75, 949.
12. Rosa, Zeiser, A., *et al.*, *Meas. Sci. Technol.* (1997) 8, 1333.
13. Mate, C. M., *et al.*, *Phys. Rev. Lett.* (1987) 59, 1942.
14. Schwarz, U. D., *et al.*, *Modern Tribology Handbook*, CRC Press, Boca Raton, FL, (2001).
15. Dienwiebel, M., *et al.*, *Phys. Rev. Lett.* (2004) 92, 126101.
16. Abel, D. G., *et al.*, *Phys. Rev. Lett.* (2007) 99, 166102.
17. Nonnenmacher, M., *et al.*, *Appl. Phys. Lett.* (1991) 58, 2921.
18. Pivetta, M., *et al.*, *Phys. Rev. Lett.* (2007) 99, 126104.
19. Hirjibehedin, C. F., *et al.*, *Science* (2007) 317, 1199.
20. Krause, S., *et al.*, *Science* (2007) 317, 1537.
21. Bode, M., *et al.*, *Nature* (2007) 447, 190.
22. Rief, M., *et al.*, *Science* (1997) 275, 1295.
23. Minne, S. C., *et al.*, *Appl. Phys. Lett.* (1998) 72, 2340.
24. Lutwyche, M., *et al.*, *Microfabrication and Parallel Operation of 5X5 2D AFM Cantilever Arrays for Data Storage and Imaging*. In: MEMS 98. Proceedings of the 11th Annual International Workshop on Micro Electro Mechanical Systems, An Investigation of Micro Structures, Sensors, Actuators, Machines and Systems, Heidelberg, January 25–29, 1998, IEEE, Los Alamitos, CA (1988).
25. Kim, Y. and Lieber, C. M., *Science* (1992) 257, 375.
26. Mesquida, P. and Stemmer, A., *Adv. Mat.* (2001) 13, 1395.
27. Guthold, M., *et al.*, *Surf. Interface Anal.* (1999) 27, 437.
28. Crommie, M. F., *et al.*, *Science* (1993) 262, 218.
29. Manoharan, H. C., *et al.*, *Nature* (2000) 403, 523.
30. Rost, M. J., *et al.*, *Phys. Rev. Lett.* (2003) 91, 026101.
31. Rost, M. J., *Phys. Rev. Lett.* (2007) 99, 266101.
32. Ando, T., *et al.*, *Proc. Natl. Acad. Sci.* (2001) 98, 12468.
33. Ando, T., *et al.*, *Pflugers Arch. – Eur. J. Physiol.* (2007) 456, 211.
34. Bryant, A., *et al.*, *Appl. Phys. Lett.* (1986) 48, 832.
35. Besenbacher, F., *et al.*, *J. Vac. Sci. Technol. B* (1990) 9, 874.
36. Ludwig, C., *et al.*, *Z. Phys. B – Condensed Matter* (1992) 86, 397.
37. Ganz, E., *et al.*, *Phys. Rev. Lett.* (1992) 68, 1567.
38. Kuipers, L., *et al.*, *Rev. Sci. Instrum.* (1995) 66, 4557.
39. Hoogeman, M. S., *et al.*, *Phys. Rev. B* (1996) 53, R13299.
40. Zambelli, T., *et al.*, *Phys. Rev. Lett.* (1996) 76, 795.
41. Wintterlin, J., *et al.*, *Surf. Sci.* (1997) 394, 159.
42. Curtis, R., *et al.*, *Rev. Sci. Instrum.* (1997) 68, 2790.
43. Linderroth, T. R., *et al.*, *Phys. Rev. Lett.* (1997) 78, 4978.
44. Horch, S., *et al.*, *Nature* (1999) 398, 134.
45. Pedersen, M. O., *et al.*, *Phys. Rev. Lett.* (2000) 84, 4898.
46. Michely, T., *et al.*, *Rev. Sci. Instrum.* (2000) 71, 4461.
47. Magnussen, O. M., *et al.*, *Electrochim. Acta* (2001) 46, 3725.
48. Petersen, L., *et al.*, *Rev. Sci. Instrum.* (2001) 72, 1438.
49. Polewska, W., *et al.*, *Electrochim. Acta* (2003) 48, 2915.
50. Labayen, M. and Magnussen, O. M., *Surf. Sci.* (2004) 573, 128.
51. Mendez, J., *et al.*, *Phys. Rev. B* (2005) 71, 085409.
52. Tansel, T. and Magnussen, O. M., *Phys. Rev. Lett.* (2006) 96, 026101.
53. Swartzentruber, B. S., *Phys. Rev. Lett.* (1996) 76, 459.
54. Pohl, D. W. and Möller, R., *Rev. Sci. Instrum.* (1988) 59, 840.
55. Aketagawa, M., *et al.*, *Rev. Sci. Instrum.* (1999) 70, 2053.
56. Hill, E., *et al.*, *Phys. Rev. B* (1999) 60, 15896.
57. Qin, X. R., *et al.*, *Phys. Rev. Lett.* (2000) 85, 3660.
58. Sato, T., *et al.*, *Surf. Sci.* (2000) 445, 130.
59. Grant, M. L., *et al.*, *Phys. Rev. Lett.* (2001) 86, 4588.
60. Rerkkumsum, P., *et al.*, *Rev. Sci. Instrum.* (2004) 75, 1061.
61. Rost, M. J., *et al.*, *Rev. Sci. Instrum.* (2005) 76, 053710.
62. Rost, M. J. and Frenken, J. W. M., *Phys. Rev. Lett.* (2001) 87, 039603.
63. Walters, D. A., *et al.*, *Proc. SPIE* (1997) 3009, 43.
64. Schäffer, T. E., *et al.*, *Proc. SPIE* (1997) 3009, 48.
65. Viani, M. B., *et al.*, *Rev. Sci. Instrum.* (1999) 70, 4300.
66. Hansma, P. K., *et al.*, *Science* (2006) 314, 601.
67. Lapshin, R. V. and Obyedkov, O. V., *Rev. Sci. Instrum.* (1993) 64, 2883.
68. Mamin, H. J., *et al.*, *J. Appl. Phys.* (1994) 75, 161.
69. Knebel, D., *et al.*, *Scanning* (1997) 19, 264.
70. Manalis, S. R., *et al.*, *Appl. Phys. Lett.* (1996) 68, 871.
71. Yamashita, H., *et al.*, *Rev. Sci. Instrum.* (2007) 78, 083702.
72. Kindt, J. H., *et al.*, *Ultramicroscopy* (2004) 100, 259.
73. Schitter, G., *et al.*, *IEEE Trans. Control Syst. Technol.* (2007) 15, 906.
74. Croft, D., *et al.*, *ASME J. Dyn. Syst. Meas. Control* (2001) 128, 35.
75. Schitter, G. and Stemmer, A., *IEEE Trans. Control Syst. Technol.* (2004) 12, 449.
76. Sebastian, A. and Salapaka, S. M., *IEEE Trans. Control Syst. Technol.* (2005) 13, 868.
77. Schitter, G., *et al.*, *Rev. Sci. Instrum.* (2001) 72, 3320.
78. Kodera, N., *et al.*, *Rev. Sci. Instrum.* (2005) 76, 053708.
79. Kodera, N., *et al.*, *Rev. Sci. Instrum.* (2006) 77, 083704.
80. Schitter, G. and Phan, N., In: *Proceedings of the 2008 American Control Conference, AACC, IEEE, Seattle, WA, (2008)*, 2690.
81. Humphris, A. D. L., *et al.*, *Appl. Phys. Lett.* (2005) 86, 034106.
82. Humphris, A. D. L., *et al.*, *Appl. Phys. Lett.* (2003) 83, 6.
83. Picco, L. M., *et al.*, *Nanotechnology* (2007) 18, 044030.
84. Fantner, G. E., *et al.*, *Rev. Sci. Instrum.* (2005) 76, 026118.
85. Gould, S. A. C., *et al.*, *J. Vac. Sci. Technol. A* (1990) 8, 369.
86. Braga, P. C. and Ricci, D., *Atomic Force Microscopy: Biomedical Methods and Applications*, 1st edn. Humana Press, Totowa, NJ, (2003).
87. Pohl, D. W., *IBM J. Res. Dev.* (1986) 30, 417.
88. Thompson, J. B., *et al.*, *Nanotechnology* (2001) 12, 394.
89. Binnig, G. K. and Smith, D. P. E., *Rev. Sci. Instrum.* (1986) 57, 1688.
90. Rost, M. J., *et al.*, *Asian J. Control* (2008) submitted.
91. <http://www.leidenprobemicroscopy.com>.
92. Disseldorp, I., *et al.*, to be published.
93. Fantner, G. E., *et al.*, *Ultramicroscopy* (2006) 106, 881.
94. Schitter, G., In: *Proceedings of the 2007 American Control Conference, AACC, IEEE, New York, (2007)*, 3503.
95. Fleming, A. J. and Moheimani, S. O. R., *IEEE Trans. Control Syst. Technol.* (2006) 14, 33.
96. Russ, C. J., *The Image Processing Handbook*, 5th edn, CRC Press, Boca Raton, FL, (2006).
97. Schitter, G., *et al.*, *Mechatronics* (2008) 18, 282.
98. Hinnen, K. J. G., *et al.*, *Proc. Inst. Mech. Engrs, Part I: J. Syst. Control Engng* (2004) 218, 503.
99. Tien, S., *et al.*, *IEEE Trans. Control Syst. Technol.* (2005) 13, 921.
100. Leang, K. K., Devasia, S., *Mechatronics* (2006) 16, 141.
101. Abramovitch, D. Y., *et al.*, In: *Proceedings of the 2007 American Control Conference, AACC, IEEE, New York, (2007)*, 3488.
102. Schitter, G., *et al.*, *Nanotechnology* (2004) 15, 108.
103. Salapaka, S., *et al.*, *Appl. Phys. Lett.* (2005) 87, 053112.